NMRlipids IV: Headgroup & glycerol backbone structures, and cation binding in bilayers with PS lipids

Pavel Buslaev,[1] Tiago M. Ferreira,[2] Ivan Gushchin,[1] Matti Javanainen,[3] Batuhan Kav,[4] Jesper J. Madsen,[5] Markus Miettinen,[4] Josef Melcr,[3] O. H. Samuli Ollila,[3,6,*] and Thomas Piggot [1.Authorlist is not yet complete][7]

[1]*Moscow Institute of Physics and Technology*
[2]*Halle, Germany*
[3]*Institute of Organic Chemistry and Biochemistry, Academy of Sciences of the Czech Republic, Prague 6, Czech Republic*
[4]*Potsdam, Germany*
[5]*Department of Chemistry, The University of Chicago, Chicago, Illinois 60637, United States of America*
[6]*Institute of Biotechnology, University of Helsinki*
[7]*Southampton, United Kingdom*

(Dated: August 10, 2018)

Phosphatidylserine (PS) is the most common negatively charged lipid in eykaryotic membranes. PS lipids interact with signaling and other proteins via electrostatic interactions and direct binding, and induce membrane fusion and phase separation together with calcium ions. Molecular details of these phenomena are not well understood because accurate models to interpret the experimental data has not been available. Here, we collect a set of experimental NMR data which could be used together with molecular dynamics (MD) simulations to interpret the lipid headgroup structures and details of ion binding in pure and mixed PS and PS:PC lipid bilayers. Aiming to interpret the data, we use the open collaboration method to go through the available MD simulation models for PS lipids. However, none of the models reproduce the experimental data with sufficient accuracy to interpet the structural details of lipid headgroups or ion binding details in lipid bilayers containing PS lipids. In contrast to PC lipids, the tested MD simulation models do not correctly reproduce the qualitative response of PS lipid headgroups to the bound ions or changes in the lipid composition. Our results pave the way for the model improvement to correctly describe negatively charged membranes and their interactions with ions.

INTRODUCTION

Phosphatidylserine (PS) is the most common negatively charged lipid in eykaryotic membranes. PS lipids compose 8.5% of total lipid weight of erythrocytes, but the abundance varies between different organelles up to 25-35% in plasma membrane [1–3]. Despite of the relatively low abundance, PS lipids are important signaling molecules. They interact with signaling proteins [2], regulate surface charge and protein localization [4], and induce protein aggregation [5, 6]. Some domains spesifically interact PS lipids, while others are attracted by general electrostatics and the binding can be regulated by calcium [2]. Therefore, the structural details of lipid headgroups and the details of cation binding are crucial for the PS mediated signaling processes.

Previous experimental studies have concluded that PS headgroups are more rigid than phophocholines (PC) due to the hydrogen bonding network or electrostatic interactions [7, 8]. Multivalent cations and Li^+ are able to form strong dehydrated molecular complexes with PS lipids, while monovalent ions interact more weakly with PS containing bilayers [9–19]. The dehydrated complexes of PS headgroup and calcium ions can also lead to the phase separation [9, 10, 14–18]. On the other hand, some studies propose that the specific binding affinity is similar to the negatively charged and zwitterionic lipids and that the increased cation binding to negatively charged lipid bilayer arise only due to the increase of local cation concentration in the vicinity of membranes [20, 21]. Dilution of bilayers with PC lipids makes PS headgroups less rigid and reduces propensity for the formation of strong complexes with multivalent ions [7, 8, 17, 18]. The molecular level interpretation of these observations is, however, not available.

Several classical molecular dynamics (MD) simulation studies are done to understand PS headgroups, their influence on lipid bilayer properties and interactions with ions [19, 22–32]. However, the recent comparisons of PC lipid headgroup and glycerol backbone C-H bond order parameters calculated from different simulation models revealed that improvements in the current force fields are needed to correctly reproduce the headgroup structure and ion binding to lipid bilayers [33–35]. The ion binding affinity to POPC bilayer was then improved by implicitly including the electronic polarizability using the electronic continuum correction [36]. Here, we collect the set of experimentally measured lipid headgroup and glycerol backbone C-H bond order parameters, which can be used to evaluate the quality of headgroup structure and the ion binding affinity in MD simulations of lipid bilayers containing PS lipids. The available MD simulation models of PS are then compared against the collected experimental data. The results pave the way for the development of MD simulation force fields that correctly describe PS lipid headgroup structure and its interactions with ions. Such models are expected to be useful in elucidating the biological role of PS and other lipid headgroups because glycerol backbone and lipid headgroups behave similarly in model membranes and in bacteria [20, 37, 38].

TABLE I: List of MD simulations of pure PS bilayers without additional salt. CKPM refers to the version with Berger/Chiu NH_3 charges compatible with Berger (i.e. the NH_3 group having the same charges as in the $N(CH_3)_3$ group of the PC lipids; 'M' stands for Mukhopadhyay after the first published Berger-based PS simulation that used these charges [24]) and CKP refers to the version with more Gromos compatible version (i.e. the charges for the NH_3 group taken from the lysine side-chain).

lipid/counter-ions	force field for lipids / ions	[a]N_l	[b]N_w	[c]N_c	[d]T (K)	[e]t_{sim}(ns)	[f]t_{anal} (ns)	[g]files
DOPS/Na^+	CHARMM36 [29]	128	4480	0	303	500	100	[39]
DOPS/Na^+	CHARMM36ua [**?**] 2.	128	4480	0	303	500	100	[40]
DOPS/Na^+	Slipids [41]	128	4480	0	303	500	100	[42]
DOPS/Na^+	Slipids [41]	288	11232	0	303	200	100	[43]
DOPS/Na^+	Berger [24]	128	4480	0	303	500	100	[44]
DOPS/Na^+	GROMOS-CKP1 [**?**] 3.	128	4480	0	303	500	100	[45]
DOPS/Na^+	GROMOS-CKP2 [**?**] 4.	128	4480	0	303	500	100	[46]
DOPS/Na^+	lipid17 [47] / JC [48]	128	4480	0	303	600	100	[49]
DOPS/Na^+	lipid17 [47] / ff99 [50]	128	4480	0	303	600	100	[51]
POPS/Na^+	CHARMM36 [29]	128	4480	0	298	500	100	[52]
POPS/K^+	CHARMM36 [29]	128	4480	0	298	500	100	[53]
POPS/Na^+	CHARMM36ua [**?**] 5.	128	4480	0	298	500	100	[54]
POPS/Na^+	Slipids [41]	128	4480	0	298	500	100	[55]
POPS/Na^+	Berger [**?**]	128	4480	0	298	500	100	[56]
POPS/Na^+	MacRog [57]	128	4480	0	298	500	100	[58]
OPPS/Na^+	MacRog [57]	128	5120	0	298	200	100	[59]
POPS/Na^+	GROMOS-CKPM [**?**] 6.	128	4480	0	298	500	100	[60]
POPS/Na^+	GROMOS-CKP [**?**] 7.	128	4480	0	298	500	100	[61]
POPS/Na^+	lipid17 [47] / JC [48]	128	4480	0	298	600	100	[62]
POPS/Na^+	lipid17 [47] / ff99 [50]	128	4480	0	298	600	100	[63]

[a]Number of lipid molecules with largest mole fraction
[b]Number of water molecules
[c]Number of additional cations
[d]Simulation temperature
[e]Total simulation time
[f]Time used for analysis
[g]Reference for simulation files

METHODS

Solid state NMR experiments

The magnitude and signs of the C-H bond order parameters in headgroup and glycerol backbone were measured using natural abundance ^{13}C solid state NMR spectroscopy as described previously [82, 83]. Shortly, the absolute values of the order parameters were determined from the dipolar splittings given by the indirect dimension of 2D R-PDFL experiment [84] and the signs were measured using S-DROSS experiments [85].

27.Details of the used spectrometer and maybe some other details should be given.

28.Sample preparation should be described.

29.How is the peak assignment done?

Molecular dynamics simulations

Molecular dynamics simulation data was collected using the Open Collaboration method [33]. The NMRlipids project blog (`nmrlipids.blogspot.fi`) and the GitHub repository (`github.com/NMRLipids/NMRlipidsIVotherHGs`) were used as the communication platforms. The simulated systems are listed in Tables I (pure PS systems without additional ions) and II (mixed PC:PS systems with various ions concentrations). Simulation details are given in the SI. The simulation data is also indexed in the searchable database (`nmrlipids.fi`), and in the NMRlipids/MATCH GitHub repository (`https://github.com/NMRLipids/MATCH`).

The C-H bond order parameters were calculated directly from the definition

$$S_{CH} = \frac{1}{2}\langle 3\cos^2\theta - 1\rangle, \quad (1)$$

where θ is the angle between the C-H bond and the membrane

TABLE II: List of POPC:POPS mixture simulations with different amounts of added ions.

8.The used definition of ion concentrations needs to be specified and standardized.

lipid/counter-ions	force field for lipids / ions	[a]C_{ci} (M)	$CaCl_2$ (M)	[b]N_l	[c]N_w	[d]N_c	[e]T (K)	[f]t_{sim}(ns)	[g]t_{anal} (ns)	[h]files
POPC:POPS (5:1)/K^+	CHARMM36 [29, 64]	0	0	110:22	4935	0	298	100	100 **9.**	[65]
POPC:POPS (5:1)/K^+	CHARMM36 [29, 64]	0	0	250:50	?	0	298	200	?	[**?**] **10.**
POPC:POPS (5:1)/K^+	CHARMM36 [29, 64]	0	0	110:22	4620	0	298	500	100	[66]
POPC:POPS (5:1)/Na^+	CHARMM36 [29, 64]	0	0	110:22	4620	0	298	500	100	[67]
POPC:POPS (1:1)/K^+	CHARMM36 [29, 64]	0	0	150:150	?	0	298	200	?	[**?**] **11.**
POPC:POPS (5:1)	CHARMM36 [29, 64, 68]	0	0.15 **12.**	250:50	?	?	298	200	?	[**?**] **13.**
POPC:POPS (5:1)	CHARMM36 [29, 64, 68]	0	1 **14.**	250:50	?	?	298	200	?	[**?**] **15.**
POPC:OPPS (5:1)/K^+	MacRog [57]	0	0	120:24	5760	0	298	200	200 **16.**	[69]
POPC:OPPS (5:1)/K^+	MacRog [57]	0	0.1	120:24	5760	10	298	200	200 **17.**	[69]
POPC:OPPS (5:1)/K^+	MacRog [57]	0	0.3	120:24	5760	31	298	200	200 **18.**	[69]
POPC:OPPS (5:1)/K^+	MacRog [57]	0	1	120:24	5760	104	298	200	200 **19.**	[69]
POPC:OPPS (5:1)/K^+	MacRog [57]	0	3	120:24	5760	311	298	200	200 **20.**	[69]
POPC:OPPS (5:1)/K^+	MacRog [57]	0.5	0	120:24	5760	52	298	200	190	[70]
POPC:OPPS (5:1)/K^+	MacRog [57]	1	0	120:24	5760	104	298	200	190	[70]
POPC:OPPS (5:1)/K^+	MacRog [57]	2	0	120:24	5760	208	298	200	145	[70]
POPC:OPPS (5:1)/K^+	MacRog [57]	3	0	120:24	5760	311	298	200	125	[70]
POPC:OPPS (5:1)/K^+	MacRog [57]	4	0	120:24	5760	415	298	200	125	[70]
POPC:POPS (5:1)/K^+	Lipid14/17 [47, 71]	0	0	120:24	5760	0	298	500	200	[72]
POPC:POPS (5:1)/K^+	Lipid14/17 [47, 71]	0.5	0	120:24	5760	?	298	300	200	[73]
POPC:POPS (5:1)/K^+	Lipid14/17 [47, 71]	1	0	120:24	5760	?	298	300	200	[73]
POPC:POPS (5:1)/K^+	Lipid14/17 [47, 71]	2	0	120:24	5760	?	298	300	200	[73]
POPC:POPS (5:1)/K^+	Lipid14/17 [47, 71]	3	0	120:24	5760	?	298	300	200	[73]
POPC:POPS (5:1)/K^+	Lipid14/17 [47, 71]	4	0	120:24	5760	?	298	300	200	[73]
POPC:POPS (5:1)/Na^+	Lipid14/17 [47, 71]	0	0	120:24	5760	0	298	500	200	[74]
POPC:POPS (5:1)/Na^+	Lipid14/17 [47, 71]	0.5	0	120:24	5760	?	298	300	200	[75]
POPC:POPS (5:1)/Na^+	Lipid14/17 [47, 71]	1	0	120:24	5760	?	298	300	200	[75]
POPC:POPS (5:1)/Na^+	Lipid14/17 [47, 71]	2	0	120:24	5760	?	298	300	200	[75]
POPC:POPS (5:1)/Na^+	Lipid14/17 [47, 71]	3	0	120:24	5760	?	298	300	200	[75]
POPC:POPS (5:1)/Na^+	Lipid14/17 [47, 71]	4	0	120:24	5760	?	298	300	200	[75]
POPC:POPS (5:1)/Na^+	Lipid14/17 [47, 71]	0	0	60:12	?	0	298	?	?	[**?**] **21.**
POPC:POPS (5:1)/Na^+	Lipid14/17 [47, 71]	0	0.03	60:12	?	0	298	?	?	[**?**] **22.**
POPC:POPS (5:1)/Na^+	Lipid14/17 [47, 71]	0	0.17	60:12	?	0	298	?	?	[**?**] **23.**
POPC:POPS (5:1)/Na^+	Lipid14/17 [47, 71]	0	0.36	60:12	?	0	298	?	?	[**?**] **24.**
POPC:POPS (4:1)/Na^+	Berger [24, 76]	0	0	102:26	4290	0	310	?	?	[**?**] **25.**
POPC:POPS (4:1)/Na^+	Berger [24, 76]**26.**	1	0	102:26	4290	80	310	200	50	[77]
POPC:POPS (4:1)	Berger [24, 76]	0	0.12	104:24	4306	24	310	300	100	[78]
POPC:POPS (4:1)	Berger [24, 76]	0	0.715	104:24	4306	72	310	300	100	[79]
POPC:POPS (5:1)/Na^+	GROMOS-CKP [**?**]	0	0	110:22	?	0	298	500	100	[80]
POPC:POPS (5:1)/Na^+	GROMOS-CKPM [**?**]	0	0	110:22	?	0	298	500	100	[81]

[a]Excess Na^+ or K^+ concentration
[b]Number of lipid molecules with largest mole fraction
[c]Number of water molecules
[d]Number of additional cations
[e]Simulation temperature
[f]Total simulation time
[g]Time used for analysis
[h]Reference for simulation files

normal. Angular brackets point to the average over all sampled configurations. **30.Error estimation should be discussed.**
The number density profiles were calculated using *gmx density* tool from Gromacs sofware package [86].

Comparison of ion binding to negatively charged lipid bilayers between simulations and experiments using the electrometer concept

The order parameters of α and β carbons in PC lipids can be used to measure the ion binding affinity because they decrease proportionally to the amound of bound positive charge to a bilayer [87–89]. This molecular electrometer concept is especially useful for the comparison between simulations and experiments because the headgroup order parameters can be directly calculated from simulations [34]. Also the headgroup order parameters of negatively charged PS and PG lipids exhibit systemic, but less characterized dependence on the bound charge [17, 90–92]. Therefore, the ion binding affinity to negatively charged bilayers can be better characterized by measuring the PC headgroup order parameters from mixed bilayers [17, 18, 92], see section S2 in the supplementary information.

Before using the PC headgroup order parameters to quantify the ion binding affinity, it is important to quantify the response of the headgroup order parameters to the known amount of bound charge [34, 36]. This can be done using the experimental data from the mixtures of monovalent cationic surfactants (dihexadecyldimethylammonium) and POPC [36, 93], see section S3 in the supplementary information. In this work, we also quantify the response of PC headgroup order parameters to the negatively charged PS headgroups, which also follows the electrometer concept in the experiments [38], see section S2 in the supplementary information.

31.How close are the hydration levels in experiments and simulations?

32.We need to decide how to report the ion concentrations, see discussion in Ref. 36.

RESULTS AND DISCUSSION

Headgroup and glycerol backbone order parameters of POPS from ^{13}C NMR

The INEPT and 2D R-PDLF experiments from POPS sample give well resolved spectras for all the carbons in headgroup and glycerol backbone region, except for g_3 for which the resolution was not sufficient to determine the numerical value of the order paramater (Fig. 1). Slices of the R-PDFL spectra (Fig. 1 C)) show a single splitting for the β-carbon with the order parameter value of 0.12, and a superposition of a large and a very small splitting for the α-carbon. The larger splitting gives a order parameter value of 0.09, while the numerical value from the small splitting cannot resolved with the available resolution. Since the R-PDFL and previous ^{2}H NMR experiments [7, 18] give only the absolute values of order parameters, we determined the signs of PS headgroup and glycerol backbone order parameters using the S-DROSS experiment [85]. The S-DROSS slice for the β-carbon (Fig. 1 D)) clearly shows that the order parameter is negative, which is confirmed by SIMPSON simulations. The beginning of the S-DROSS slice suggests that the higher order parameter of the α-carbon is positive and the deviation towards negative values with the longer T_1 times suggests that the smaller order parameter is negative. This is confirmed by a SIMPSON simulation where the value of -0.02 was taken from ^{2}H NMR experiment [18] for the smaller order parameter. The literature value was used because the resolution of our experiment was not sufficient to determine the small value of the order parameter. The S-DROSS curve from SIMPSON simulation with a positive value for the smaller order parameter (dashed grey in Fig. 1 D)) did not agree with the experiment, confirming the interpretation that the smaller order parameter is negative.

The headgroup and glycerol backbone order parameters of POPS measured in this work are in good agreement with the previously reported values from ^{2}H NMR experiments of DOPS [7] (Fig. 2). The β-carbon order parameter is significantly more negative and α-carbon experiences a significant forking in PS headgroup when compared with the values previously measured for POPC [82] (Fig. 2). These features have been intepreted to arise from a rigid PS headgroup conformation, stabilized by hydrogen bonds or electrostatic interactions [7, 8], but detailed structrural interpretation is not available.

Headgroup and glycerol backbone in simulations of PS lipid bilayers without additional ions

None of the tested models reproduce the experimental headgroup and glycerol backbone order parameters of DOPS and POPS within the experimental error bars (Fig. 3). The tested models perform generally less well than the models tested for PC headgroup in the previous study (Fig. 2 in Ref. [33]), which is also evindent from the comparison between subjective rankings of the model quality for the headgroup and glycerol backbone (Fig. 4 and Fig. 4 in Ref. [33]). Therefore, the models cannot be straightforwardly used to interpret the structural differences between PC and PS headgroups. However, the differences are partially reproduced by the two best performing models for the α and β-carbons of PS headgroups, Slipids and CHARMM36. Both reproduce the larger forking of the α-carbon and the Slipids model reproduces also the lower of the β-carbon order in parameter in the PS headgroups (Fig. 3 and Fig. 2 in Ref. 33). Interestingly, the dihedral angle distributions in these two models share significant similarities in the headgroup region (Fig. S7). **37.Notation of dihedrals in Fig. S7 should be made somehow combatible with the chemical structures in Fig. 2 and the discussion should be then finished.** However, the glycerol backbone order parameters in Slipids model significantly differ from CHARMM36 results and experiments (Fig. 3), which can be related to the differences in the dihedral angle distributions of C1-C2-C3-O31 and C2-C3-O31-

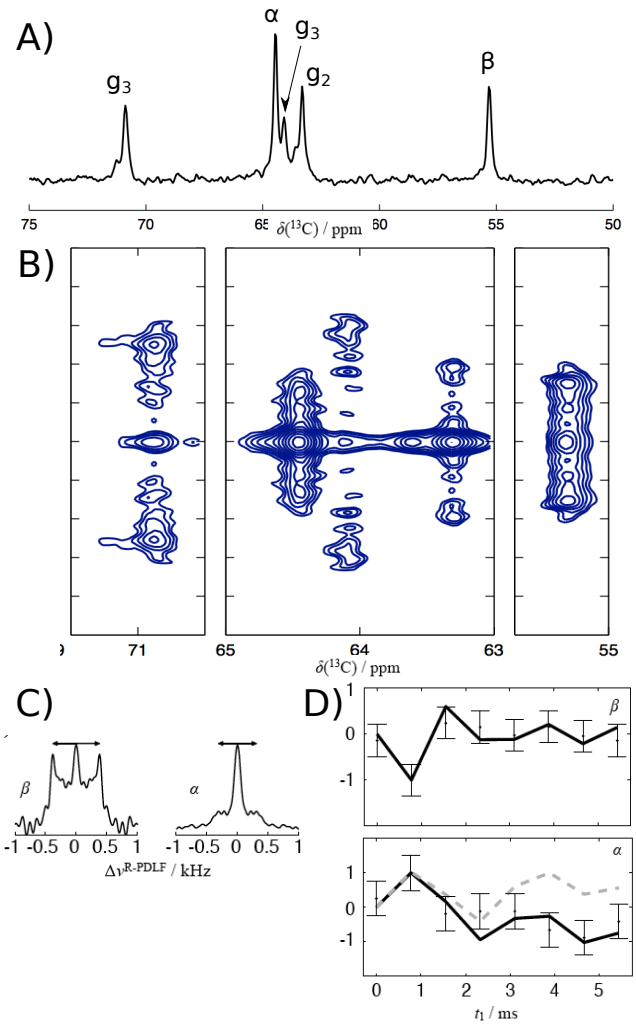

FIG. 1: (a) The headgroup region of the INEPT spectrum with headgroup and glycerol backbone carbons assigned. (b) 2D R-PDLF spectra for headgroup and glycerol backbone regions. (c) Slices for α and β barbons. (d) Experimental SDROSS data (points) and SIMPSON simulations (lines). Order parameter values of -0.12 for the β-carbon, and 0.09 and -0.02 for the larger and smaller α-carbon slittings were used in the SIMPSON calculations. The S-DROSS curve from SIMPSON simulation with positive value for the smaller order parameter (dashed grey).

33.This is preliminary figure, should be polished.

34.Should we show slices for all the analyzed carbons in (c)?

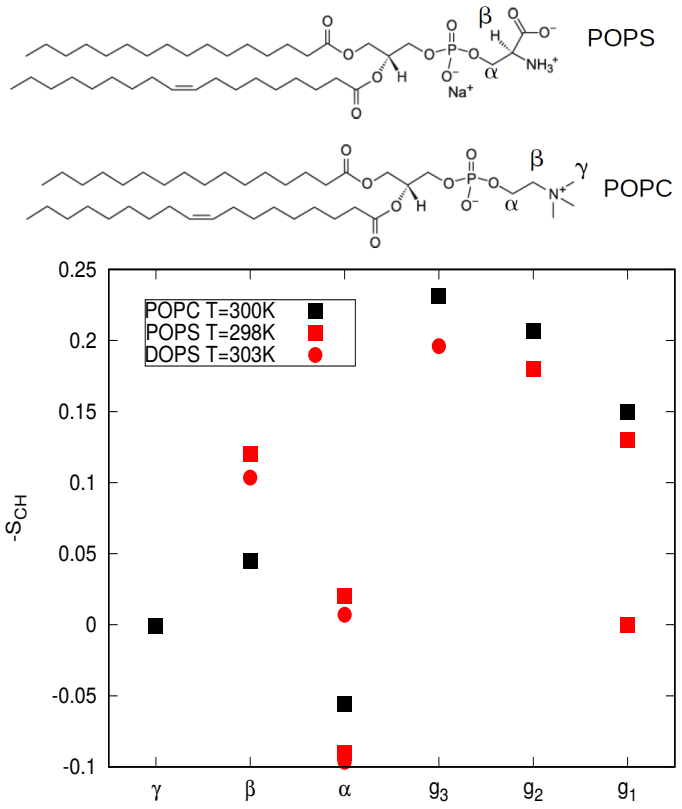

FIG. 2: Headgroup and glycerol backbone order parameters of POPS measured in this work compared with the values from DOPS (^{2}H NMR, 0.1M of NaCl) [7] and POPC (^{13}C NMR) [82] experiments. Signs of the PS order parameters are measured in this work. Signs of the PC order parameters are measured in Ref. [83].

C31 (Fig. S6). Similar difference was previously observed for PC lipids [33] and the conformational differences are illustrated in Figure S8.

38.POPS/OPPS issue with MacRog model is in progress: https://github.com/NMRLipids/NMRlipidsIVotherHGs/issues/16

Counterion binding to lipid bilayers containing PS lipids

Membranes containing PS lipids are always accomppanied with counterions, which modulate electrostatic interactions between lipids and other biomolecules. Counterions are also suggested screen the repulsion between charged lipid headgroups in MD simulations and reduce the area per lipid of PS bilayers to be smaller than in PC bilayers [23–25]. The counterion density profiles along membrane normal show significant differences between simulation models (Fig. 6). The strongest counterion binding, i.e., the lowest concentrations in bulk water, are observed in MacRog, Berger and Lipid17/JC simulations. CHARMM36, CHARMM36ua and Gromos-CKP models exhibit two local maxima in counterion density, while a single maxima is observed in the other models. **39.More detailed discussion may be possible after comparing monovalent ion binding to bilayers between CHARMM simulations and experiments. Also, section S6 should be finished.** Area per lipid is in agreement with experiments [30] only in the Gromos-CKP models, while other models give significantly lower values (Fig. 6). The difference cannot be explained by the electrostatic screening of the headgroup repulsion due to counterion binding because CHARMM36, CHARMM36ua and Slipid models give smaller area per lipid than Gromos-CKP models with similar counterion binding affinity.

To evaluate counterion binding in different simulation models against experimental data [17], we plot the headgroup or-

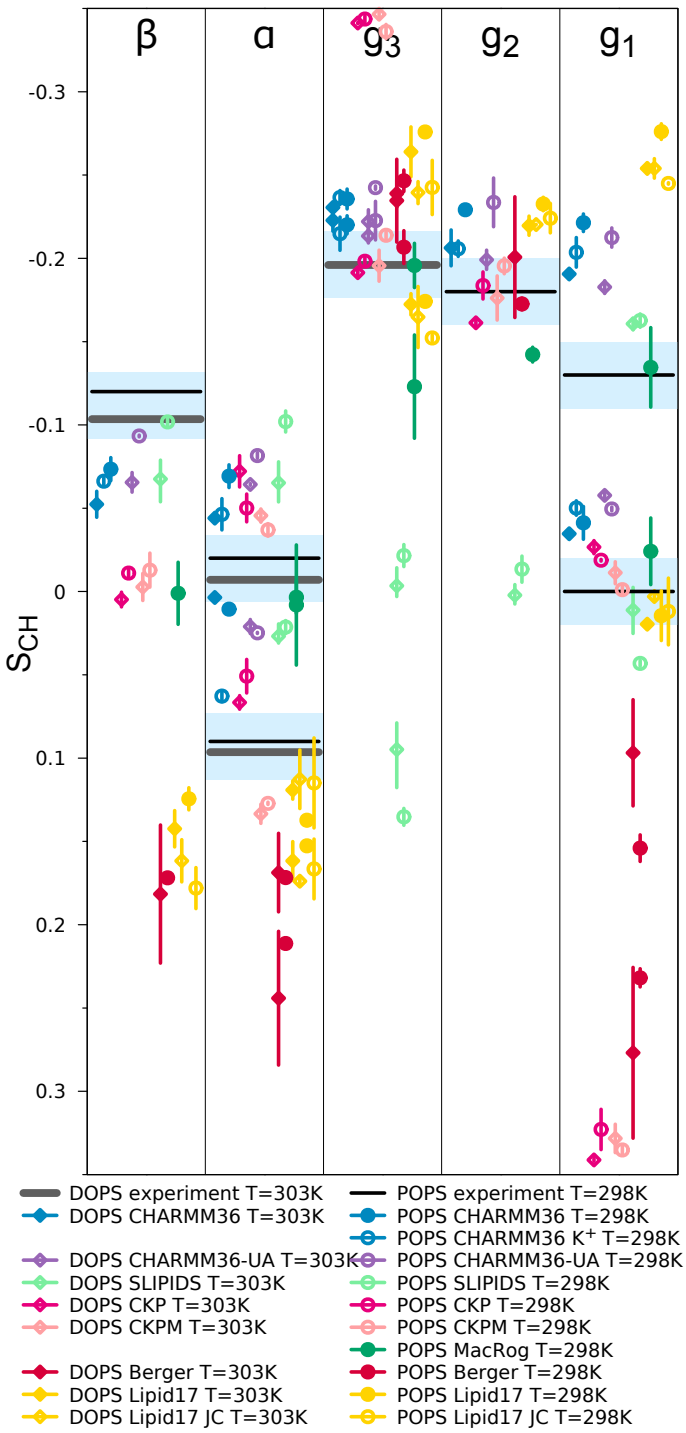

FIG. 3: Order parameters for PS headgroup and glycerol backbone from simulations with different models and experiments without $CaCl_2$. All DOPS data at 303 K, POPS at 298 K. Experimental data from [7] contain 0.1 M of NaCl. Signs are taken from experiments for POPS described in Supplementary Information. The vertical bars shown are not error bars, but demonstrate that we had at least two data sets; the ends of the bars mark the extreme values from the sets, and the dot marks their measurement-time-weighted average.

	β	α	g_3	g_2	g_1	Σ
CHARMM 36	M	M F	M	M	**M** F	8
CHARMM 36-UA	M	M	M	M	**M** F	8
GROMOS-CKP1	**M**	M **F**	**M F**		**M F**	14
GROMOS-CKP2	**M**	M F	**M F**		**M F**	14
Slipid	M	**M**	**M F**	**M**	M **F**	14
Berger	**M**	**M F**	M F	M	**M** F	15

FIG. 4: Rough subjective ranking of force fields based on Figure 3. Here ÒMÓ indicates a magnitude problem, ÒFÓ a forking problem; letter size increases with problem severity. Color scheme: Òwithin experimental errorÓ (dark green), Òalmost within experimental errorÓ (light green), Òclear deviation from experimentsÓ (light red), and Òmajor deviation from experimentsÓ (dark red). The Σ-column shows the total deviation of the force field, when individual carbons are given weights of 0 (matches experiment), 1, 2, and 4 (major deviation). For full details of the assessment, see Supplementary Information.

35.Issue about possible updates to this plot:
https://github.com/NMRLipids/NMRlipidsIVotherHGs/issues/4
36.Lipid17 and MacRog results should be added into this plot.

der parameters measured from POPC:POPS 5:1 mixture as a function of different monovalent ions added to the buffer (Fig. 7). Experimental order parameter data for POPC headgroup in the mixture is available as a function of LiCl and KCl concentrations, while POPS headgroup order parameters are measured also as a function of NaCl. Lithium interacts more strongly with PS headgroups than other monovalent ions [12, 14, 16, 17, 92], as also observed for PC headgroups [94]. This is evident also in the changes of PS headgroup order parameters, which decrease with the addition of lithium but increase with the addition of sodium or potassium (Fig. 7). POPC headgroup order parameters exhibit a clear decrease as a function of LiCl concentration but only modest changes as a function of KCl concentration, indicating singificant Li^+ binding but only weak Na^+ binding to the mixture when interpreted using the electrometer concept [87–89]. In simulations with the Berger model, the headgroup order parameter response of POPC to the added NaCl is similar to the experiments of LiCl, indicating overestimated binding affinity of sodium, in line with the results for PC bilayers [34]. Indeed, the sodium density profile shows a significant binding

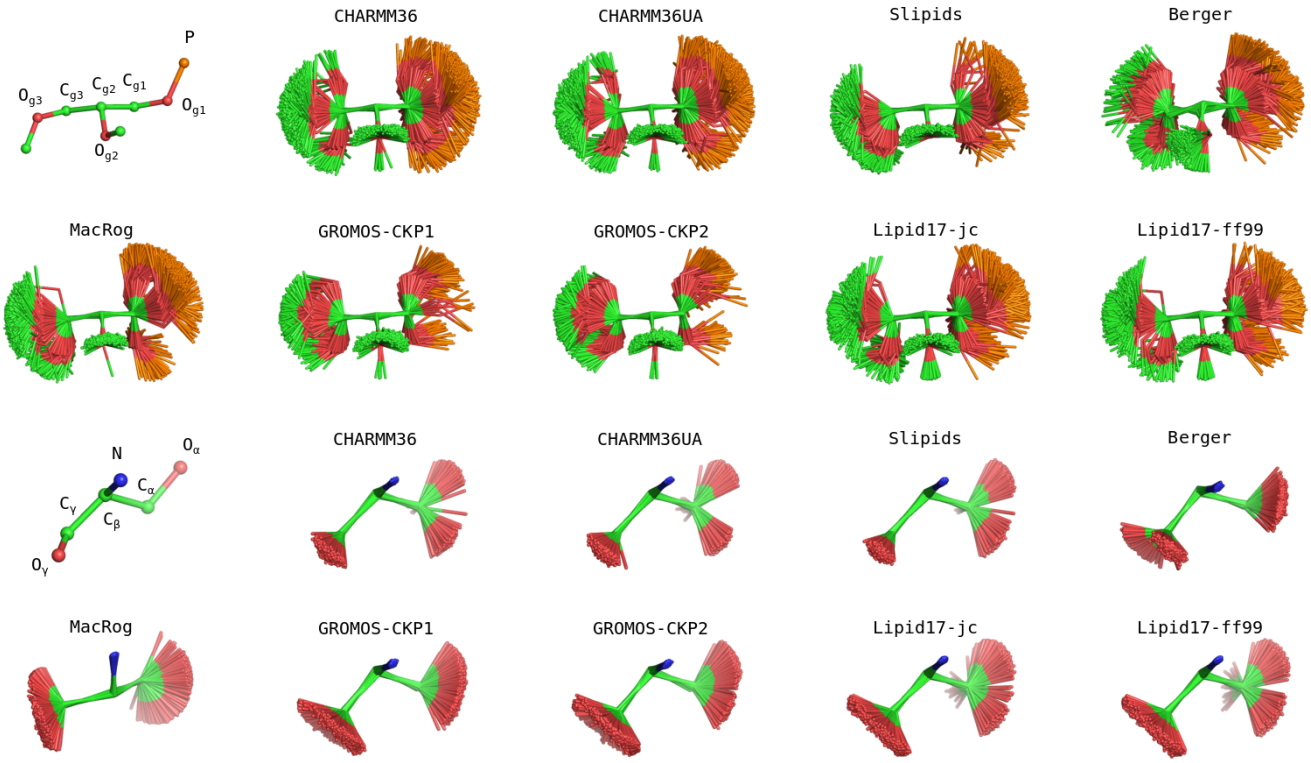

FIG. 5: Overlayed snapshots from glycerol backbone and headgroup region from different simulations of PS lipids.

peak in the Berger model (Fig. 8). Potassium binding in the MacRog simulation is significantly weaker (Fig. 8) and the headgroup order parameter changes are also in better agreement with simulations (Fig. 7). **40.Discussion about Lipid17 to be written when we have the density profiles.** All the tested models overestimate the changes of POPS headgroup order parameters as a function of monovalent ions (Fig. 7), suggesting that model development is necessary to interpret the PS headgroup-ion interactions from MD simulations.

Headgroup structure in PS and PC mixtures

Dilution of PS lipid bilayers with PC lipids reduces the propensity of PS headgroup-multivalent ion complexes and is proposed to make PS headgroups less rigid [7, 8, 17, 18]. Therefore, the intermolecular interactions at the headgroup region seems to be important for the physical properties of mixed lipid bilayers. These interactions can be indirectly monitored by measuring the headgroup order parameters from PS:PC mixtures with different molar ratios. The headgroup order parameters of POPC increase in such experiments with increasing amount of POPS (Fig. 9) [38]. This behaviour is generally observed when negatively charged lipids or surfactants are mixed with PC lipids [38, 93] and can be understood by the tilting of lipid headgroup more parallel to the membrane plane according to the electrometer concept [89]. The headgroup order parameters of PS lipids shift closer to zero when bilayer is diluted with PC lipids in experiments (Fig. 9) [7, 17, 38], which is intepreted to indicate reduced rigidity [7, 8].

The increase of POPC headgroup order parameters with the increasing amount of negatively charged POPS lipid is reproduced in MacRog simulations with potassium counterions, but not in Berger simulations with sodium or in CHARMM36 simulations with potassium or sodium conterions (Fig. 9). The observations can be explained using the electrometer concept. The Berger simulation exhibits very strong sodium binding (Fig. 8), which surpasses the effect of negatively charged lipids as also the amount of counterions increase with increasing amount of PS. In CHARMM36 simulations, the counterion binding neutralizes the effect of PS and the headgroup order parameters are not changed with increasing amount of PS. Finally, the weak binding of potassium in the MacRog simulations enables the increase of order parameters with the increasing amount of negatively charged PS lipids (Figs. 9 and 8).

Oppositely to experiments, the headgroup order parameter of POPS shift away from zero in CHARM36 simulations when bilayer is diluted with POPC (Fig. 9). In lipid14/17 simulations, the POPS order parameter shift closer to zero when bilayer is diluted with POPC, but the numerical values of order parameters are too far from experiments to enable interpretation of the experimental data. Therefore, we conlcude that the force field development is necessary before MD sim-

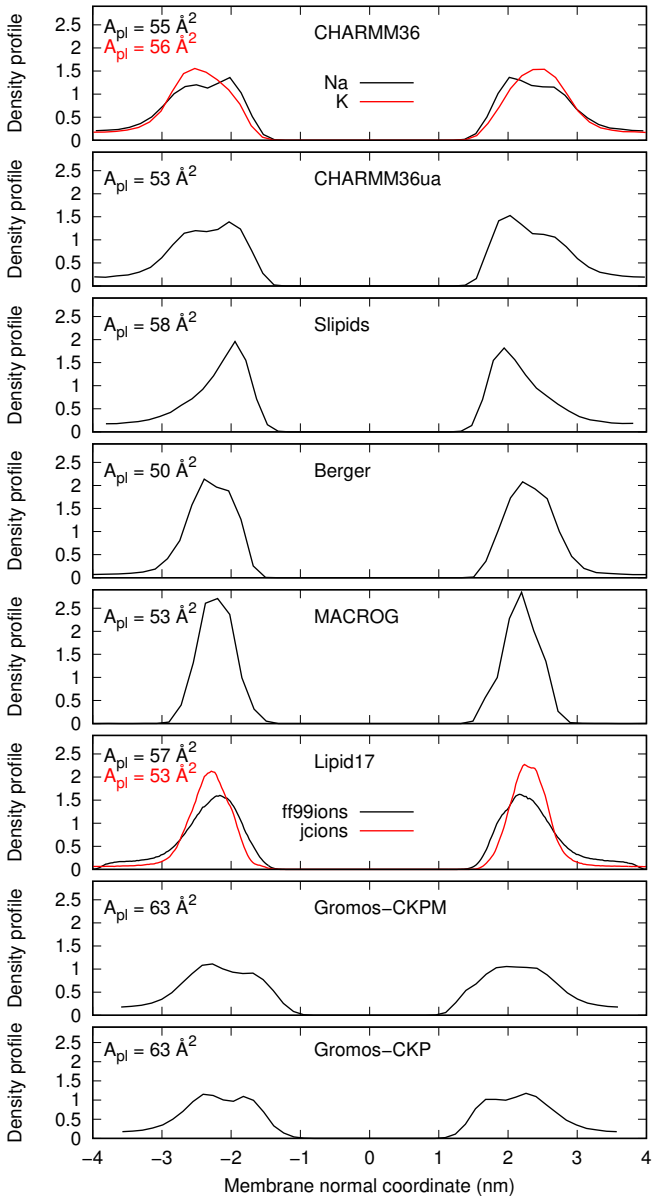

FIG. 6: Counterion densities of POPS lipid bilayer along the membrane normal from simulations with different force fields.

ulations can be used to interpret the interactions between PC and PS headgroups.

Ca^{2+} binding affinity in bilayers with negatively charged PS lipids

Ion binding affinity to PS containing membranes can be most conveniently measured from PC:PS lipid mixtures where the lipid-ion complexes and phase separation are not observed [15–18]. Also, the headgroup order parameters of PC can be used to detect ion binding affinity to the mixed lipid bilayers, see section S2. As expected from the previous study of PC lipid bilayers [34], the decrease of POPC headgroup order parameters in POPC:POPS mixtures as a function of Ca^{2+} concentration is overestimated with respect to experiments [17] in almost all the tested simulation models (Fig. 10), indicating overestimated calcium binding binding affinity. Only exception is the CHARMM36 model with the special NBfix [68] interaction, incorporated in the parameters give by the CHARMM-GUI at the time of running the simulations (January 2018), which underestimates the calcium binding affinity. With this interaction, the calcium and sodium binding affinities to POPC bilayer are equally weak (see section S7), in contrast to experimental data [87, 88, 94]. Therefore, we conclude that the ion binding peaks in density distributions along membrane normal (Fig. 11) are underestimated in the CHARMM36/NBfix model, but overestimated in the other tested models.

The headgroup order parameters of POPS headgroup measured from POPC:POPS (5:1) mixture exhibit a strong dependence of $CaCl_2$ with small concentrations with a rapid saturation below 100 mM (Fig. 10). The β-carbon order parameter of POPS increase with the added $CaCl_2$ in the experiment and in all the tested simulation models, but simulations significantly overestimated the change. The larger α-carbon order parameter of POPS decrease and the smaller one slightly increase with the added $CaCl_2$ in the experiment. The changes are again significantly overestimated in the simulations, however, in this case all simulations predict qualitatively different behaviour. Notably, the changes of POPS headgroup order parameters are overestimated also in the CHARMM36/NBfix model where the calcium binding affinity was too low. We conclude that the effect of bound ions to the headgroup order parameters of POPS is not qualitatively reproduced by the tested simulations models. This is in contrast to previous results for PC headgroup [34], where qualitatively correct reponse to bound ions was observed despite of significant discrepancies in the headgroup structure without additional ions. The response of POPS headgroup order parameters to the bound charge is systematic but less well understood than the responce of PC headgroups used in the electrometer concept [17, 89]. The force field development is necessary to generate MD simulations that could be used to explain the interactions between PS headgroup and calcium ions.

CONCLUSIONS

We have collected a set of experimental NMR order parameter data, which could be combined with MD simulations to interpret the headgroup structure and cation binding details to negatively charged membranes containing PS lipids. Using open collaboration method, we tried to find a MD simulation model which would be sufficiently accurate to interpret the experimental data. However, none of the tested models was accurate enough. In line with the previous study for PC lipids [34], MD simulation models seems to generally overes-

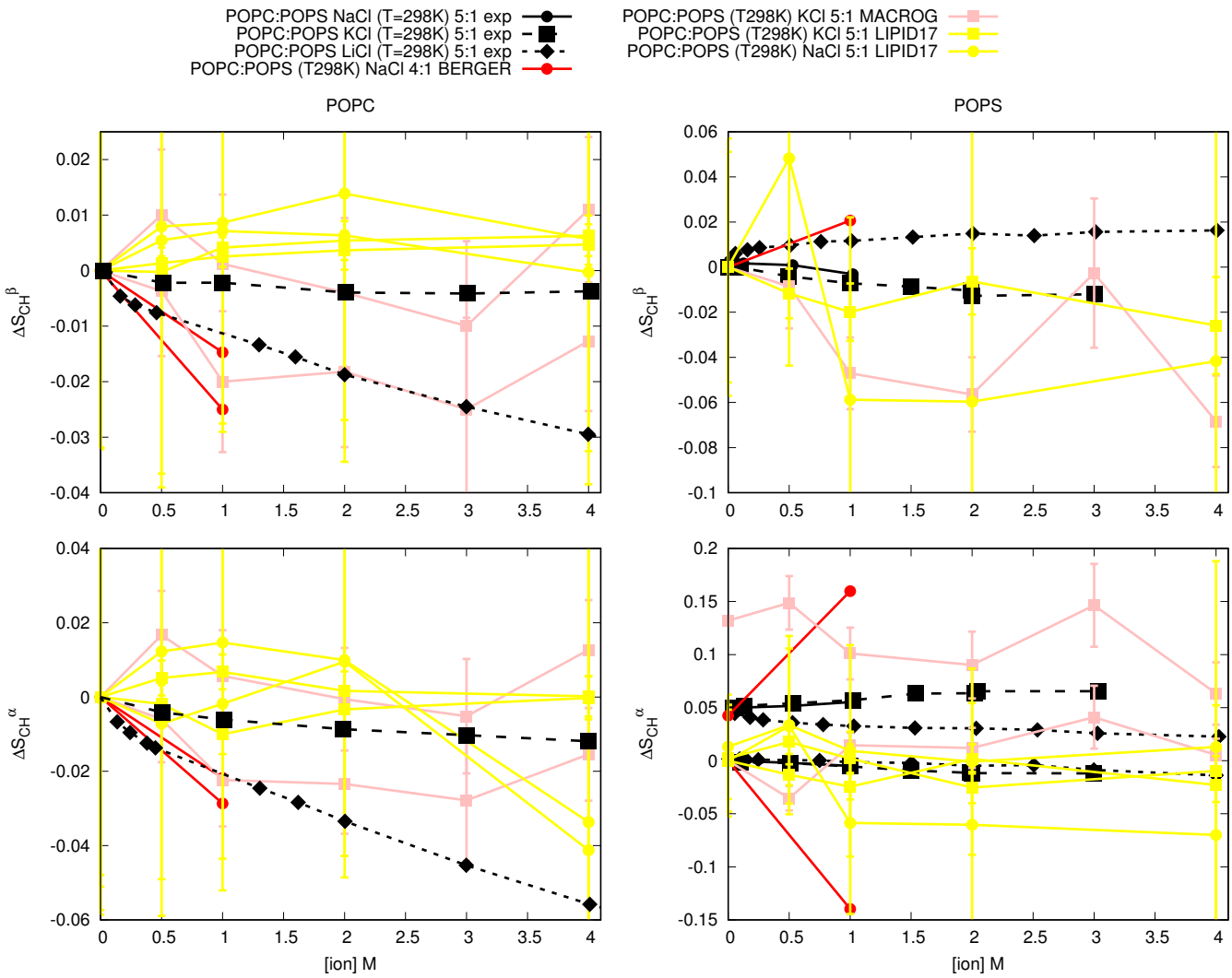

FIG. 7: Changes of the PC (left) and PS (right) headgroup order parameters as a function of added NaCl, KCl and LiCl from POPC:POPS (5:1) mixture. The experimental data is from Ref. 17. The values from counterion-only systems are set as a zero point of y-axis. To correctly illustrate the significant forking of the α-carbon order parameter in PS headgroup (bottom, right), the y-axis is tranferred with the same value for both order parameters such that the lower order parameter value is at zero.

41.CHARMM36 results for this plot would be highly useful.

timate cation binding also to negatively charged bilayers containing PS lipids, with some exceptions. The response of PS lipid headgroup order parameters to the bound cations does not agree with experiments, even in the cases where binding affinity is not overestimated. This is in contrast to the previous results with PC lipids, where the qualitative response of the headgroup order parameters was in agreement with experiments even in the cases where the headgroup structure without ions was not correct and the cation binding affinity was overestimated. In addition, the inaccurate responses of PS headgroup order parameters to the dilution with PC lipids suggests that the PC-PS interactions are not accurately described by the tested models.

Our results pave the way for improving the PS lipid parameters for MD simulations by offering the set of experimental data for the quality measurement, by pinpointing problems areas in the models and suggesting directions for the corrections. Improvements using the electronic continuum correction is already in progress `https://github.com/jmelcr/ecc_lipids`, following the recent work for PC lipids [36].

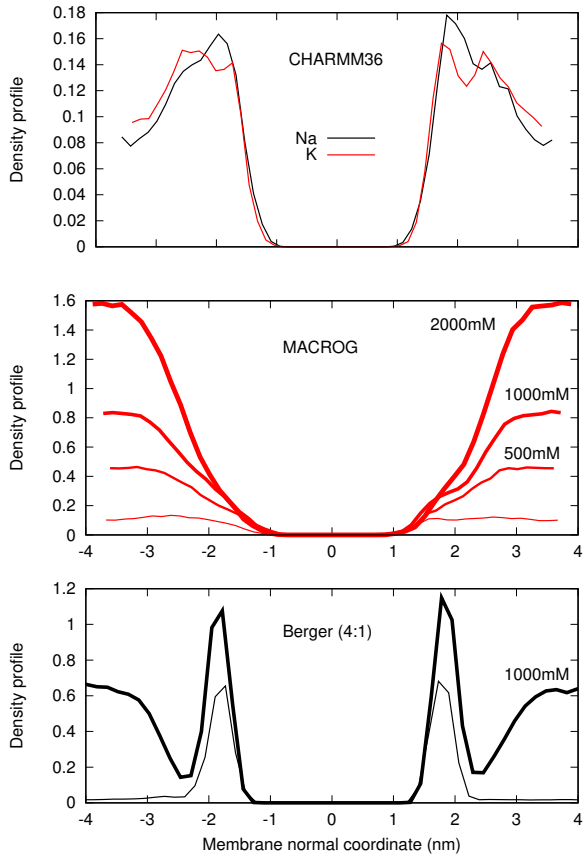

FIG. 8: Counterion density distributions from PC:PS mixtures.

42.Lipid 17 is to be added.

* samuli.ollila@helsinki.fi

[1] M. A. Lemmon, Nat. Rev. Mol. Cell Biol. **9**, 99 (2008).

[2] P. A. Leventis and S. Grinstein, Annual Review of Biophysics **39**, 407 (2010).

[3] L. Li, X. Shi, X. Guo, H. Li, and C. Xu, Trends in Biochemical Sciences **39**, 130 (2014), ISSN 0968-0004.

[4] T. Yeung, G. E. Gilbert, J. Shi, J. Silvius, A. Kapus, and S. Grinstein, Science **319**, 210 (2008).

[5] H. Zhao, E. K. J. Tuominen, and P. K. J. Kinnunen, Biochemistry **43**, 10302 (2004).

[6] G. P. Gorbenko and P. K. Kinnunen, Chemistry and Physics of Lipids **141**, 72 (2006).

[7] J. L. Browning and J. Seelig, Biochemistry **19**, 1262 (1980).

[8] G. Büldt and R. Wohlgemuth, The Journal of Membrane Biology **58**, 81 (1981), ISSN 1432-1424, URL http://dx.doi.org/10.1007/BF01870972.

[9] H. Hauser, E. Finer, and A. Darke, Biochemical and Biophysical Research Communications **76**, 267 (1977), ISSN 0006-291X, URL http://www.sciencedirect.com/science/article/pii/0006291X77907215.

[10] R. J. Kurland, Biochemical and Biophysical Research Communications **88**, 927 (1979), ISSN 0006-291X, URL http://www.sciencedirect.com/science/article/pii/0006291X79914979.

[11] M. Eisenberg, T. Gresalfi, T. Riccio, and S. McLaughlin, Biochemistry **18**, 5213 (1979).

[12] H. Hauser and G. G. Shipley, Biochemistry **22**, 2171 (1983).

[13] R. Dluhy, D. G. Cameron, H. H. Mantsch, and R. Mendelsohn, Biochemistry **22**, 6318 (1983).

[14] H. Hauser and G. Shipley, Biochimica et Biophysica Acta (BBA) - Biomembranes **813**, 343 (1985), ISSN 0005-2736, URL http://www.sciencedirect.com/science/article/pii/0005273685902512.

[15] G. W. Feigenson, Biochemistry **25**, 5819 (1986).

[16] J. Mattai, H. Hauser, R. A. Demel, and G. G. Shipley, Biochemistry **28**, 2322 (1989).

[17] M. Roux and M. Bloom, Biochemistry **29**, 7077 (1990).

[18] M. Roux and M. Bloom, Biophys. J. **60**, 38 (1991).

[19] J. M. Boettcher, R. L. Davis-Harrison, M. C. Clay, A. J. Nieuwkoop, Y. Z. Ohkubo, E. Tajkhorshid, J. H. Morrissey, and C. M. Rienstra, Biochemistry **50**, 2264 (2011).

[20] J. Seelig, Cell Biology International Reports **14**, 353 (1990), ISSN 0309-1651, URL http://www.sciencedirect.com/science/article/pii/030916519091204H.

[21] C. G. Sinn, M. Antonietti, and R. Dimova, Colloids and Surfaces A: Physicochemical and Engineering Aspects **282-283**, 410 (2006), a Collection of Papers in Honor of Professor Ivan B. Ivanov (Laboratory of Chemical Physics and Engineering, University of Sofia) Celebrating his Contributions to Colloid and Surface Science on the Occasion of his 70th Birthday.

[22] J. J. López Cascales, J. García de la Torre, S. J. Marrink, and H. J. C. Berendsen, The Journal of Chemical Physics **104**, 2713 (1996).

[23] S. A. Pandit and M. L. Berkowitz, Biophysical Journal **82**, 1818 (2002).

[24] P. Mukhopadhyay, L. Monticelli, and D. P. Tieleman, Biophysical Journal **86**, 1601 (2004).

[25] U. R. Pedersen, C. Leidy, P. Westh, and G. H. Peters, Biochimica et Biophysica Acta (BBA) - Biomembranes **1758**, 573 (2006).

[26] P. T. Vernier, M. J. Ziegler, and R. Dimova, Langmuir **25**, 1020 (2009).

[27] A. Martín-Molina, C. Rodríguez-Beas, and J. Faraudo, Biophysical Journal **102**, 2095 (2012).

[28] P. Jurkiewicz, L. Cwiklik, A. Vojtíšková, P. Jungwirth, and M. Hof, Biochimica et Biophysica Acta (BBA) - Biomembranes **1818**, 609 (2012).

[29] R. M. Venable, Y. Luo, K. Gawrisch, B. Roux, and R. W. Pastor, The Journal of Physical Chemistry B **117**, 10183 (2013).

[30] J. Pan, X. Cheng, L. Monticelli, F. A. Heberle, N. Kucerka, D. P. Tieleman, and J. Katsaras, Soft Matter **10**, 3716 (2014).

[31] S. Vangaveti and A. Travesset, The Journal of Chemical Physics **141**, 245102 (2014).

[32] A. Melcrová, S. Pokorna, S. Pullanchery, M. Kohagen, P. Jurkiewicz, M. Hof, P. Jungwirth, P. S. Cremer, and L. Cwiklik, Sci. Reports **6**, 38035 (2016).

[33] A. Botan, F. Favela-Rosales, P. F. J. Fuchs, M. Javanainen, M. Kanduč, W. Kulig, A. Lamberg, C. Loison, A. Lyubartsev, M. S. Miettinen, et al., J. Phys. Chem. B **119**, 15075 (2015).

[34] A. Catte, M. Girych, M. Javanainen, C. Loison, J. Melcr, M. S. Miettinen, L. Monticelli, J. Maatta, V. S. Oganesyan, O. H. S. Ollila, et al., Phys. Chem. Chem. Phys. **18**, 32560 (2016).

[35] O. S. Ollila and G. Pabst, Biochimica et Biophysica Acta (BBA) - Biomembranes **1858**, 2512 (2016).

[36] J. Melcr, H. Martinez-Seara, R. Nencini, J. Kolafa, P. Jung-

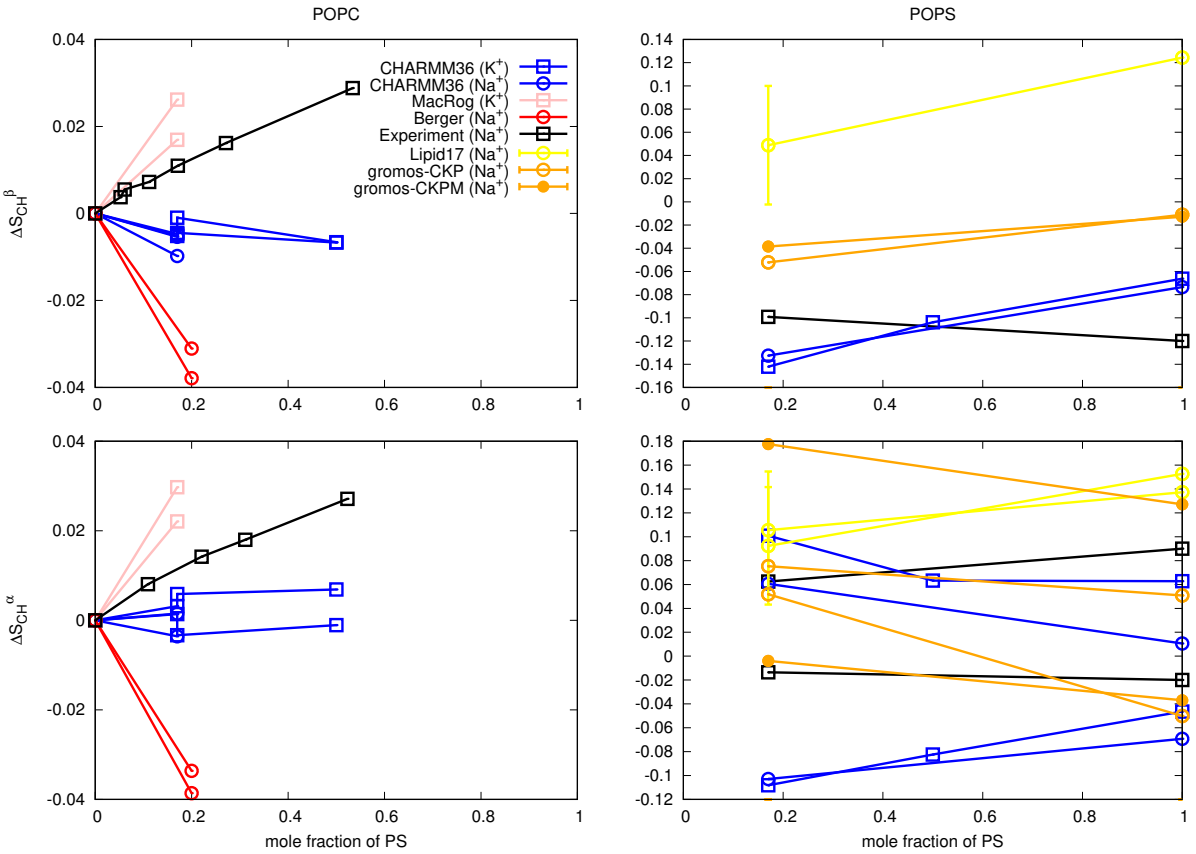

FIG. 9: Changes of PC (left panel) and PS (right panel) headgroup order parameters from POPC:POPS mixtures with increasing amount of POPS. Experimental results of POPC are taken from Ref. 38 (signs are determined as discussed in [33, 35]). Experimental values for POPS in pure bilayer and in mixture are measured in this work and in Ref. 17 at 298K, respectively. Since the experimental data of POPS in pure and diluted mixture come from different experimental sets (13C NMR in this work and 2H NMR from Ref. 17), the experimental change of the order parameter is less accurate than in typical measurements where same technique is used in all conditions, see discussion about qualitative and quantitative accuracy in Ref. 35. For POPC (left panel) the zero point of y-axis is set to the value of pure bilayer. For β-carbon of POPS (right panel, top) the zero point of y-axis is set to the value from POPC:POPS (5:1) mixture. For α-carbon of POPS (right panel, bottom) the y-axis is tranferred with the same value for both order parameters such that the lower order parameter value from POPC:POPS (5:1) mixture is at zero to correctly illustrate the significant forking.

43.Simulation of CHARMM36 at 298K should be maybe rerun with Gromacs 5.

44.Simulation of pure POPC at 298K with Lipid14 would be useful for this plot (only at 303 K is available from NMRlipids I)

45.MacRog simulations of pure POPS with potassium counterions only would be useful for this and other plots.

46.The data from POPC used in Gromos-CKP by would be useful for this plot.

wirth, and O. H. S. Ollila, The Journal of Physical Chemistry B **122**, 4546 (2018).

[37] H. U. Gally, G. Pluschke, P. Overath, and J. Seelig, Biochemistry **20**, 1826 (1981).

[38] P. Scherer and J. Seelig, EMBO J. **6** (1987).

[39] T. Piggot, *CHARMM36 DOPS simulations (versions 1 and 2) 303 K 1.0 nm LJ switching* (2017), URL `https://doi.org/10.5281/zenodo.1129411`.

[40] T. Piggot, *CHARMM36-UA DOPS simulations (versions 1 and 2) 303 K 1.0 nm LJ switching* (2017), URL `https://doi.org/10.5281/zenodo.1129456`.

[41] J. P. M. Jämbeck and A. P. Lyubartsev, Phys. Chem. Chem. Phys. **15**, 4677 (2013).

[42] T. Piggot, *Slipids DOPS simulations (versions 1 and 2) 303 K 1.0 nm cut-off with LJ-PME* (2017), URL `https://doi.org/10.5281/zenodo.1129439`.

[43] F. Favela-Rosales, *MD simulation trajectory of a fully hydrated DOPS bilayer: SLIPIDS, Gromacs 5.0.4. 2017.* (2017), URL `https://doi.org/10.5281/zenodo.495510`.

[44] T. Piggot, *Berger DOPS simulations (versions 1 and 2) 303 K 1.0 nm cut-off* (2017), URL `https://doi.org/10.5281/zenodo.1129419`.

[45] T. Piggot, *GROMOS-CKP DOPS simulations (versions 1 and 2) 303 K with Berger/Chiu NH3 charges and PME* (2017), URL `https://doi.org/10.5281/zenodo.1129429`.

[46] T. Piggot, *GROMOS-CKP DOPS simulations (versions 1 and 2) 303 K with GROMOS NH3 charges and PME* (2017), URL `https://doi.org/10.5281/zenodo.1129447`.

[47] I. Gould, A. Skjevik, C. Dickson, B. Madej, and R. Walker, *Lipid17: A comprehensive amber force field for the simulation of zwitterionic and anionic lipids* (2018), in preparation.

[48] I. S. Joung and T. E. Cheatham, The Journal of Physical Chem-

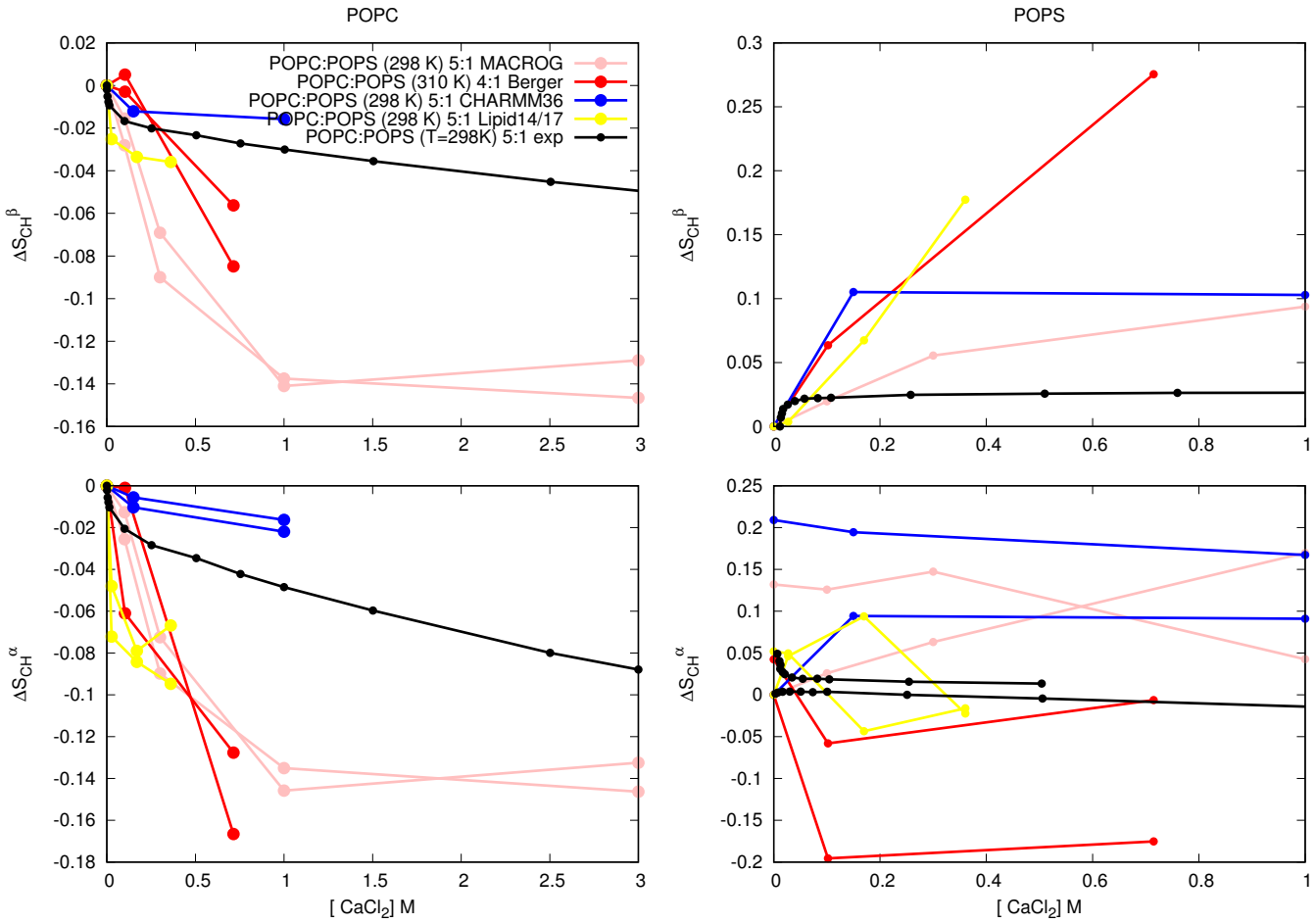

FIG. 10: Changes of POPC (left) and POPS (right) headgroup order parameters in POPC:POPS (5:1) mixture as a function $CaCl_2$ concentration. Experimental data is taken from 17. The values from counterion-only systems are set as a zero point of y-axis. To correctly illustrate the significant forking of the α-carbon order parameter in PS headgroup (bottom, right), the y-axis is tranferred with the same value for both order parameters such that the lower order parameter value is at zero.

47.Information about the cuonterions in different simulations should be added

48.Upcoming simulations with original CHARMM36 have been mentioned in the blog:

http://nmrlipids.blogspot.com/2017/12/nmrlipids-iv-current-status-and.html?showComment=1520090718976#c5569269391707740056

49.Upcoming Lipid17 simulations have been mentioned in the blog

http://nmrlipids.blogspot.com/2017/12/nmrlipids-iv-current-status-and.html?showComment=1515177306419#c994825612316235467

istry B **112**, 9020 (2008).

[49] B. Kav and M. S. Miettinen, *Molecular dynamics simulation trajectory of an anionic lipid bilayer: 100 mol% DOPS with Na+ counterions using Joung-Cheetham Ions* (2018), B.K acknowledges financial support from International Max Planck Research School on Multiscale Bio-Systems, URL `https://doi.org/10.5281/zenodo.1134871`.

[50] J. Åqvist, J. Phys. Chem. **94**, 8021 (1990).

[51] B. Kav and M. S. Miettinen, *Molecular dynamics simulation trajectory of an anionic lipid bilayer: 100 mol% DOPS with Na+ counterions using ff99 Ions* (2018), B.K acknowledges financial support from International Max Planck Research School on Multiscale Bio-Systems, URL `https://doi.org/10.5281/zenodo.1135142`.

[52] T. Piggot, *CHARMM36 POPS simulations (versions 1 and 2) 298 K 1.0 nm LJ switching* (2017), URL `https://doi.org/10.5281/zenodo.1129415`.

[53] T. Piggot, *CHARMM36 POPS simulations (versions 1 and 2) 298 K 1.0 nm LJ switching with K ions* (2018), URL `https://doi.org/10.5281/zenodo.1182654`.

[54] T. Piggot, *CHARMM36-UA POPS simulations (versions 1 and 2) 298 K 1.0 nm LJ switching* (2017), URL `https://doi.org/10.5281/zenodo.1129458`.

[55] T. Piggot, *Slipids POPS simulations (versions 1 and 2) 298 K 1.0 nm cut-off with LJ-PME* (2017), URL `https://doi.org/10.5281/zenodo.1129441`.

[56] T. Piggot, *Berger POPS simulations (versions 1 and 2) 298 K 1.0 nm cut-off* (2017), URL `https://doi.org/10.5281/zenodo.1129425`.

[57] A. Maciejewski, M. Pasenkiewicz-Gierula, O. Cramariuc, I. Vattulainen, and T. Róg, J. Phys. Chem. B **118**, 4571 (2014).

[58] T. Piggot, *MacRog POPS simulations (versions 1 and 2) 298 K*

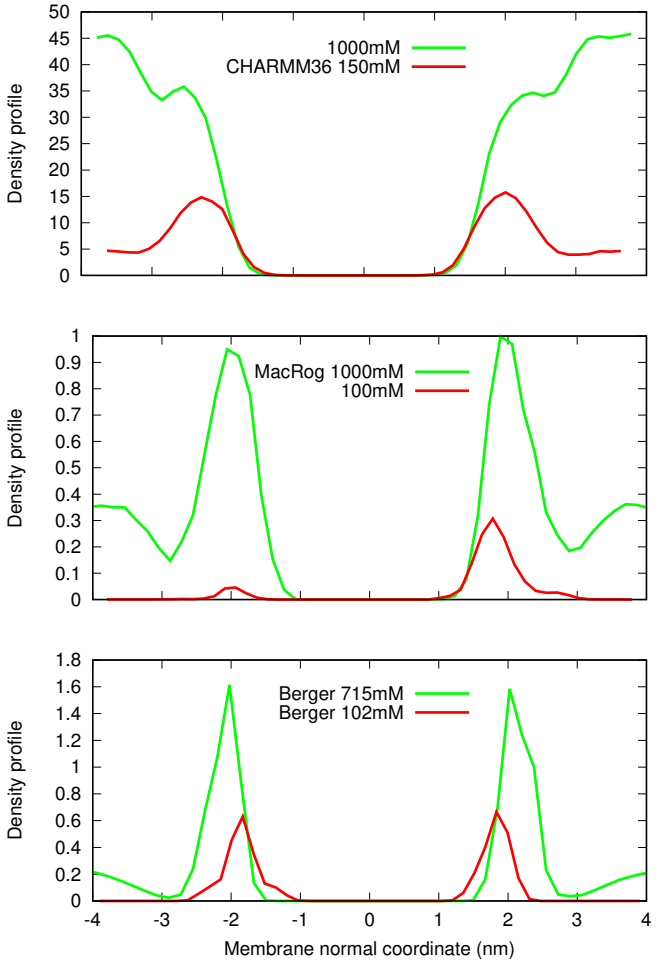

FIG. 11: Ca2+ density profiles from simulations.

50.The CHARMM results are mass densities, numbers should be used.

51.Should we include also counterions into the plot?

52.Not all the data from MacRog is included.

with corrected PO not OP tails (2018), URL https://doi.org/10.5281/zenodo.1283335.

[59] M. Javanainen, *Simulation of a pops bilayer* (2017), URL https://doi.org/10.5281/zenodo.1120287.

[60] T. Piggot, *GROMOS-CKP POPS simulations (versions 1 and 2) 298 K with Berger/Chiu NH3 charges and PME* (2017), URL https://doi.org/10.5281/zenodo.1129431.

[61] T. Piggot, *GROMOS-CKP POPS simulations (versions 1 and 2) 298 K with GROMOS NH3 charges and PME* (2017), URL https://doi.org/10.5281/zenodo.1129435.

[62] M. S. Miettinen and B. Kav, *Molecular dynamics simulation trajectory of an anionic lipid bilayer: 100 mol% POPS with Na+ counterions using Joung-Cheatham Ions* (2018), B.K. acknowledges financial support from International Max Planck Research School on Multiscale Bio-Systems., URL https://doi.org/10.5281/zenodo.1148495.

[63] M. S. Miettinen and B. Kav, *Molecular dynamics simulation trajectory of an anionic lipid bilayer: 100 mol% POPS with Na+ counterions using ff99 ions* (2018), B.K. acknowledges financial support from International Max Planck Research School on Multiscale Bio-Systems, URL https://doi.org/10.5281/zenodo.1134869.

[64] J. B. Klauda, R. M. Venable, J. A. Freites, J. W. O'Connor, D. J. Tobias, C. Mondragon-Ramirez, I. Vorobyov, A. D. MacKerell Jr, and R. W. Pastor, J. Phys. Chem. B **114**, 7830 (2010).

[65] O. H. S. Ollila, *POPS+83%popc lipid bilayer simulation at T298K ran CHARMM_GUI force field and Gromacs* (2017), URL https://doi.org/10.5281/zenodo.1011104.

[66] T. Piggot, *CHARMM36 POPS/POPC simulations (versions 1 and 2) 298 K 1.0 nm LJ switching with K ions* (2018), URL https://doi.org/10.5281/zenodo.1182658.

[67] T. Piggot, *CHARMM36 POPS/POPC simulations (versions 1 and 2) 298 K 1.0 nm LJ switching with Na ions* (2018), URL https://doi.org/10.5281/zenodo.1182665.

[68] S. Kim, D. Patel, S. Park, J. Slusky, J. Klauda, G. Widmalm, and W. Im, Biophysical Journal **111**, 1750 (2016), ISSN 0006-3495, URL http://www.sciencedirect.com/science/article/pii/S0006349516307615.

[69] M. Javanainen, *Simulations of popc/pops membranes with cacl_2.* (2017), URL https://doi.org/10.5281/zenodo.897467.

[70] M. Javanainen, *Simulations of popc/pops membranes with kcl* (2018), URL https://doi.org/10.5281/zenodo.1210256.

[71] C. J. Dickson, B. D. Madej, A. A. Skjevik, R. M. Betz, K. Teigen, I. R. Gould, and R. C. Walker, J. Chem. Theory Comput. **10**, 865 (2014).

[72] B. Kav and M. S. Miettinen, *Amber Lipid17 Simulations of POPC/POPS Membranes with KCl Counterions* (2018), B.K acknowledges financial support from International Max Planck Research School on Multiscale Bio-Systems, URL https://doi.org/10.5281/zenodo.1250969.

[73] B. Kav and M. S. Miettinen, *Amber Lipid17 Simulations of POPC/POPS Membranes with KCl* (2018), B.K acknowledges financial support from International Max Planck Research School on Multiscale Bio-Systems, URL https://doi.org/10.5281/zenodo.1227257.

[74] B. Kav and M. S. Miettinen, *Amber Lipid17 Simulations of POPC/POPS Membranes with NaCl Counterions* (2018), B.K acknowledges financial support from International Max Planck Research School on Multiscale Bio-Systems, URL https://doi.org/10.5281/zenodo.1250975.

[75] B. Kav and M. S. Miettinen, *Amber Lipid17 Simulations of POPC/POPS Membranes with NaCl* (2018), B.K acknowledges financial support from International Max Planck Research School on Multiscale Bio-Systems, URL https://doi.org/10.5281/zenodo.1227272.

[76] D. P. Tieleman, H. J. Berendsen, and M. S. Sansom, Biophys. J. **76**, 1757 (1999).

[77] L. Cwiklik, *MD simulation trajectory of a POPC/POPS (4:1) bilayer with 1M NaCl, Berger force field for lipids and ffgmx for ions* (2017), URL https://doi.org/10.5281/zenodo.838219.

[78] C. Lukasz, *MD simulation trajectory of a POPC/POPS (4:1) bilayer with 102mM CaCl2, Berger force field for lipids, scaled charges for Ca2+ and Cl-* (2017), URL https://doi.org/10.5281/zenodo.887398.

[79] C. Lukasz, *MD simulation trajectory of a POPC/POPS (4:1) bilayer with 715mM CaCl2, Berger force field for lipids, scaled charges for Ca2+ and Cl-* (2017), URL https://doi.org/10.5281/zenodo.887400.

[80] T. Piggot, *GROMOS-CKP POPS/POPC simulations (versions 1 and 2) 298 K with GROMOS NH3 charges and PME* (2018), URL https://doi.org/10.5281/zenodo.1283333.
[81] T. Piggot, *GROMOS-CKP POPS/POPC simulations (versions 1 and 2) 298 K with Berger/Chiu NH3 charges and PME* (2018), URL https://doi.org/10.5281/zenodo.1283331.
[82] T. M. Ferreira, F. Coreta-Gomes, O. H. S. Ollila, M. J. Moreno, W. L. C. Vaz, and D. Topgaard, Phys. Chem. Chem. Phys. **15**, 1976 (2013).
[83] T. M. Ferreira, R. Sood, R. Bärenwald, G. Carlström, D. Topgaard, K. Saalwächter, P. K. J. Kinnunen, and O. H. S. Ollila, Langmuir **32**, 6524 (2016).
[84] S. V. Dvinskikh, H. Zimmermann, A. Maliniak, and D. Sandstrom, J. Magn. Reson. **168**, 194 (2004).
[85] J. D. Gross, D. E. Warschawski, and R. G. Griffin, J. Am. Chem. Soc. **119**, 796 (1997).
[86] M. Abraham, D. van der Spoel, E. Lindahl, B. Hess, and the GROMACS development team, *GROMACS user manual version 5.0.7* (2015), URL www.gromacs.org.
[87] H. Akutsu and J. Seelig, Biochemistry **20**, 7366 (1981).
[88] C. Altenbach and J. Seelig, Biochemistry **23**, 3913 (1984).
[89] J. Seelig, P. M. MacDonald, and P. G. Scherer, Biochemistry **26**, 7535 (1987).
[90] F. Borle and J. Seelig, Chemistry and Physics of Lipids **36**, 263 (1985).
[91] P. M. Macdonald and J. Seelig, Biochemistry **26**, 1231 (1987).
[92] M. Roux and J.-M. Neumann, FEBS Letters **199**, 33 (1986).
[93] P. G. Scherer and J. Seelig, Biochemistry **28**, 7720 (1989).
[94] G. Cevc, Biochim. Biophys. Acta - Rev. Biomemb. **1031**, 311 (1990).

ToDo